Supporting Information

Scale-Up of Microdroplet Reactions by Heated Ultrasonic Nebulization

Chengyuan Liu[a, ‡], Jia Li[a, ‡], Hao Chen[b], Richard N. Zare[a,*]

---

[a]   Department of Chemistry, Fudan University, Shanghai 200438, China

[b]   Department of Chemistry & Environmental Science, New Jersey Institute of Technology, Newark, NJ 07102, USA

‡   C.Y. Liu and J. Li contributed equally to this work.

*   To whom correspondence should be addressed: rnz@fudan.edu.cn

Table of Contents

Section 1: Reaction procedures

Claisen-Schmidt condensation

For HUN microdroplet reaction, it was performed by first mixing 0.4 mL of 50 mM benzaldehyde (in methanol), 0.4 mL of 50 mM 6-hydroxy-1-indanone (in methanol) and 0.4 mL of 1.8 M methanolic KOH and then nebulizing the reaction mixture in the nebulization cell. In bulk reaction, 1 mL of 50 mM 6-hydroxy-1-indanone, 1 mL of 50 mM benzaldehyde, and 1 mL of 1.8 M base were mixed and stirred at 50 °C.

Oximation reaction

For HUN microdroplet synthesis of ketoxime, 0.5 mL of 50 mM benzophenone in the methanol and 0.5 mL of 1 M hydroxylamine in 1 M methanolic NaOH were mixed and nebulized in the nebulization cell. Bulk reaction was performed by mixing 2 mL of 50 mM benzophenone and 2 mL of 1 M hydroxylamine in methanolic NaOH at 50 °C.

Two-phase oxidation reaction

The two-phase reaction was performed without the use of phase-transfer-catalyst (PTC). For the two-phase HUN microdroplet synthesis of 4-methoxybenzaldehyde, 0.5 mL of 200 mM 4-methoxybenzyl alcohol in ethyl acetate (EtOAc) and 0.6 mL of aqueous NaClO (11-14%) were mixed and nebulized in the nebulization cell at 50 °C. The bulk reaction was performed by mixing 2 mL of 200 mM 4-methoxybenzyl alcohol and 2.4 mL of aqueous NaClO (11-14%) at 50 °C.

Eschenmoser coupling reaction

At first, following a previous procedure,[1] 1-methylpyrrolidine-2-thione was synthesized. N-methyl-2-pyrrolidone (11.6 mmol, 1.0 eq) was dissolved in CH_2Cl_2 (0.50 M), added to a flask containing Lawesson's reagent (0.5 eq, 0.25 M in CH_2Cl_2), stirred and the progress of the reaction was monitored by TLC. The volatiles were removed under reduced pressure and the resulting crude product was purified by silica gel column chromatography eluting with ethylacetate/petroleum (80/20), yield 94%.

For microdroplet and bulk reaction, 87 mM 1-methylpyrrolidine-2-thione, 130 mM diethyl bromomalonate (1.5 eq) and 87 mM Na_2CO_3 (1 eq) were mixed in 1 mL CH_3CN/H_2O (v:v=9:1). For both instances, the temperature was kept at 50 °C for 3.5 min.

Section 2: General information and analysis methods

General Information

Reagents and solvents were used as received without further purification. Benzaldehyde (99 %), 6-hydroxy-1-indanone (98 %), benzophenone (99 %), benzophenone oxime (98 %), 4-methoxybenzyl alcohol (98 %), 4-methoxybenzaldehyde(99 %) and diethyl bromomalonate (98 %) were purchased from Adamas Reagent Co., Ltd. (Shanghai, China). Potassium hydroxide (KOH, AR grade, $\geqslant$85 %), sodium hydroxide (NaOH, AR grade, $\geqslant$96 %), ethyl acetate (EtOAc) ($\geqslant$99.5 %) and sodium carbonate (Na_2CO_3, 99.95%) were bought from Greagent (Shanghai, China). Hydroxylamine solution (50 wt.% in H_2O) and 11-14 % sodium hypochlorite (NaClO) solution were purchased from Energy Chemical (Shanghai, China) and Alfa Aesar Co., Inc. (USA), respectively. HPLC grade methanol and acetonitrile was purchased from Fisher (Waltham, MA). Ultra-pure water was prepared by Millipore Milli-Q Advantage A10 Water Purification System (Bedford, MA, USA).

Instrumentation and method

A LTQ XL Orbitrap hybrid instrument (Thermo Fisher Scientific, Bremen, Germany) was used for the nanoESI-MS analysis of Claisen-Schmidt condensation samples in the negative ion mode. The distance between the tip of the spray emitter and ion transfer capillary to the MS was held constant at ca. 1 mm and a spray voltage of negative 1.5 kV was used. All samples were diluted 10-fold with methanol prior to mass analysis. MS data were analyzed using the Qual Browser feature of the Xcalibur™ program (Thermo Fisher Scientific). The size of microdroplets in nebulization cell was measured by a laser diffractometer (Sympatec HELOS, Sympatec, Germany).

An Agilent 1260 high-performance liquid chromatography with diode-array detection (HPLC/DAD) (Agilent, USA) was used to analyze the samples of oximation reaction, two-phase reaction and Eschenmoser coupling reaction. A C18 column (5 μm, 4.6 mm i.d. × 150 mm) was utilized for HPLC analysis with 1 mL min⁻¹ of methanol−water, containing 0.1% trifluoroacetic acid, as mobile phase. The oximation reaction and two-phase reaction were monitored by using a UV detection wavelength of 254 nm and the Eschenmoser coupling reaction was detected at 280 nm. Prior to analysis, the samples of oximation reaction, two-phase reaction and Eschenmoser coupling reaction were diluted 20-fold, 20-fold and 100-fold, respectively. The data analysis was performed using Chemstation software.

The byproducts of two-phase reaction in the bulk phase were identified and characterized by gas chromatography mass spectrometry (PE680-ST8, PerkinElmer, America) and ¹H NMR spectrometer (Avance III-HD 400 MHz, Bruker-Biospin, USA). The prepared reactant (1-methylpyrrolidine-2-thione) and product (enaminone) in the Eschenmoser coupling reaction was also characterized by ¹H NMR spectrometer.

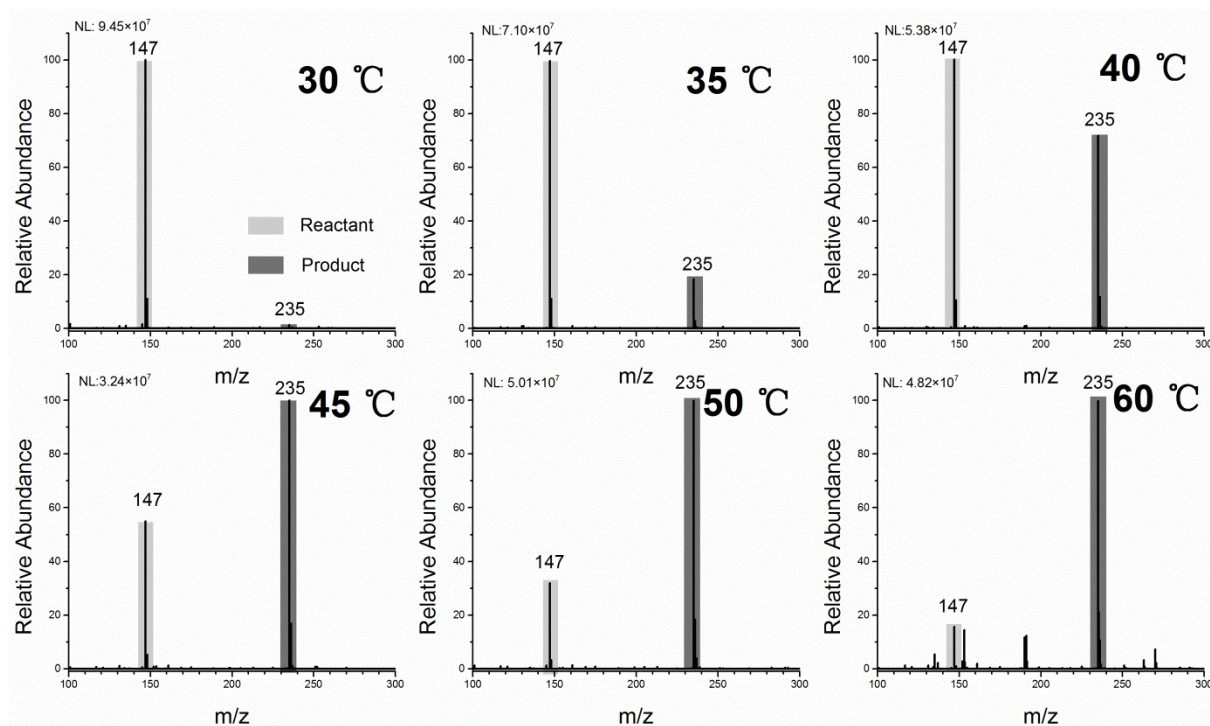## Section 3: The influence of temperature, reaction time and volume

Figure S1. Influence of temperature on the HUN microdroplet reaction of the Claisen-Schmidt condensation
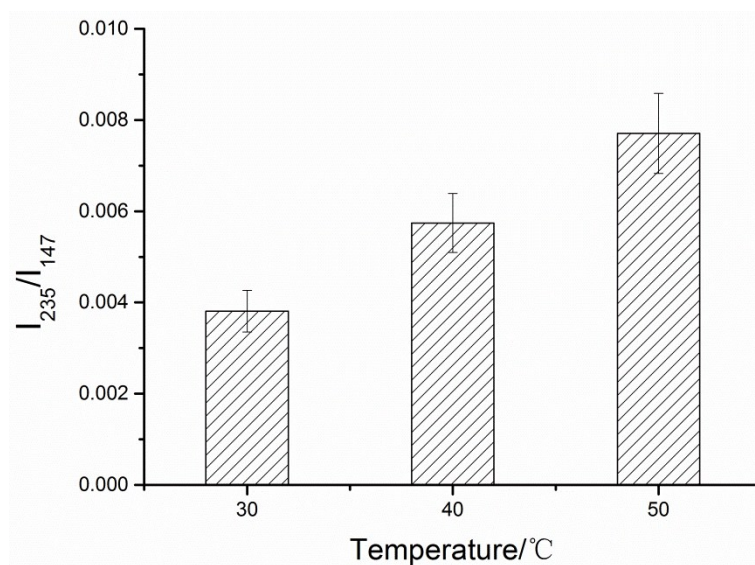

Figure S2. The effect of temperature on the product/reactant ratio in the Claisen-Schmidt condensation reaction in bulk phase.
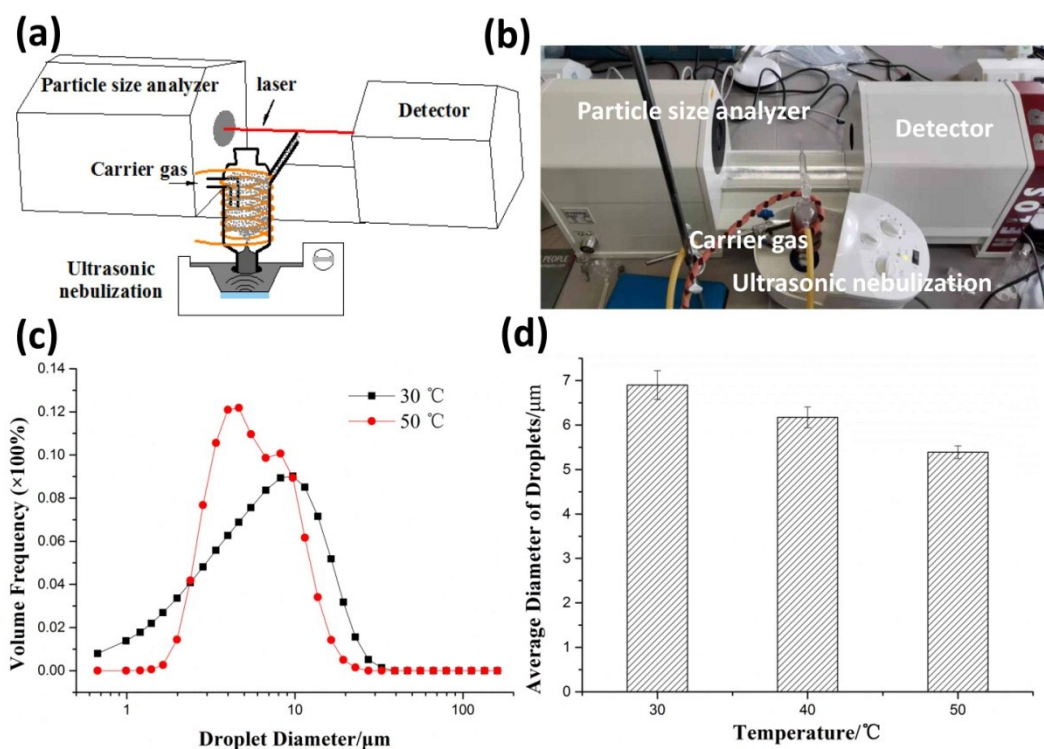
b

Figure S3. (a) The schematic diagram and (b) picture of the experimental setup which was used for the detection of the droplet diameter in HUN system. The droplets in the ultrasonic nebulization cell were delivered by carrier gas to the detection zone of a laser diffractometer (Sympatec HELOS, Sympatec, Germany). (c) The droplet size distributions of methanol solvent at 30 °C and 50 °C; (d) the average diameters of droplets of methanol solvent in HUN at different temperatures.
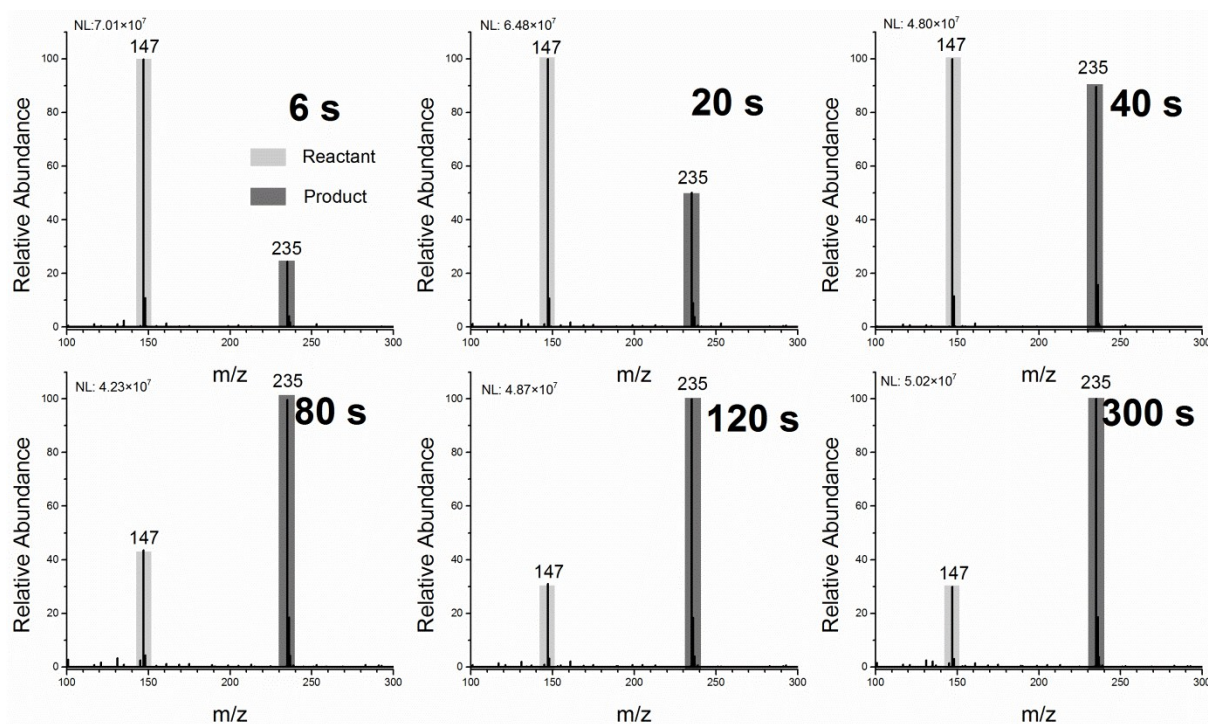

Figure S4. Influence of reaction time on the HUN microdroplet reaction of the Claisen-Schmidt condensation.
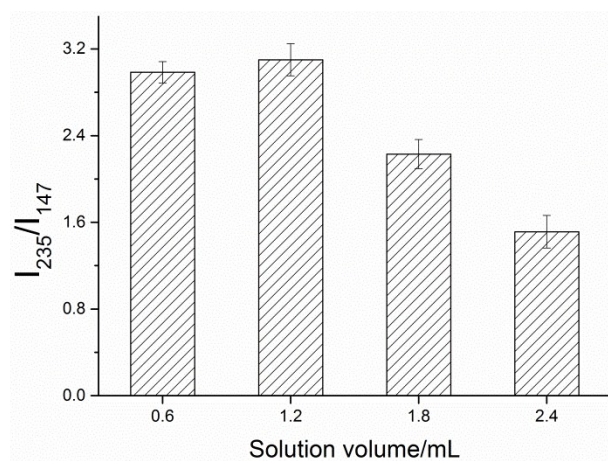
Figure S5. Influence of the volume of reactant solution in nebulization cell on the HUN microdroplet reaction of the Claisen-Schmidt condensation.

Section 4: Kinetic calculations for bulk and microdroplet reaction

Claisen-Schmidt condensation

The remaining concentration of reactant (6-hydroxy-1-indanone) at a certain reaction t was calculated as follows:

$$\frac{I_{147}}{I_{235}} = \frac{C_t \times R_i}{C_0 - C_t} \qquad (1)$$

where I_{147} and I_{235} represent MS ion intensity of reactant (6-hydroxy-1-indanone) and product (6-hydroxy-2-benzyliden-1-indanone) at *m/z* 147 and 235 respectively; C_0 and C_t represent the initial concentration and remaining concentration of reactant (6-hydroxy-1-indanone); R_i represents the ratio of ionization efficiency of reactant and product.

$$\frac{I_{147}}{I_{235}} = \frac{C_{reactant}}{C_{product}} R_i \qquad (2)$$

$C_{reactant}$ and $C_{product}$ are the concentrations of reactant and product. From Eq. 2, R_i is the slope of the calibration plots of ion intensity ratio vs concentration ratio. Please note that in order to keep consistent with the condensation reaction solution, 60 mM KOH was added in the mixture of reactant and product. According to the plot in Figure S6, *Ri* for the reactant and product in the Claisen-Schmidt condensation is 2.2.
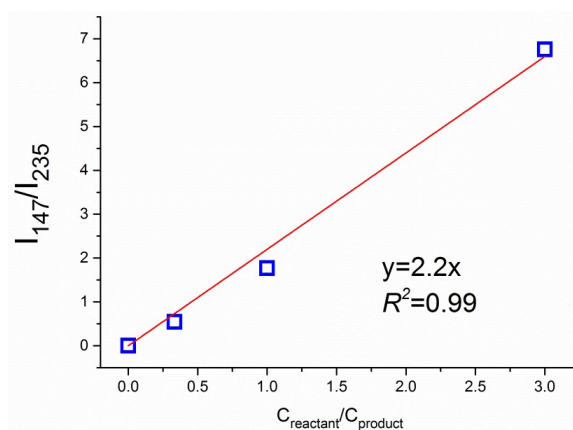

Figure S6. Standard calibration plots for ion intensity ratio vs. concentration ratio of reactant and product for the Claisen-Schmidt condensation obtained by negative ion mode mass spectrometry.

In our experiment, the concentration of 6-hydroxy-1-indanone and benzaldehyde were the same so that the condensation reaction takes place as a second-order reaction. The reaction rate constant *k* can be derived by plotting $1/C_t$ vs time as following Eq. 3.

$$\frac{1}{C_t} = kt + b \qquad (3)$$

Oximation reaction

The remaining concentration of reactant (benzophenone) at a certain reaction t was calculated as follows:

$$\frac{A_{benzophenone}}{A_{benzophenone\ oxime}} = \frac{C_t \times R_{a1}}{C_0 - C_t} \qquad (4)$$

where $A_{benzophenone}$ and $A_{benzophenone\ oxime}$ represent UV absorption of reactant (benzophenone) and product (benzophenone oxime) at the detection wavelength of 254 nm; C_0 and C_t represent the initial concentration and remaining concentration of reactant (benzophenone); R_{a1} represents the ratio of absorption efficiency of benzophenone and benzophenone oxime.

$$\frac{A_{benzophenone}}{A_{benzophenone\ oxime}} = \frac{C_{benzophenone}}{C_{benzophenone\ oxime}} R_{a1} \qquad (5)$$

$C_{benzophenone}$ and $C_{benzophenone\ oxime}$ are the concentrations of benzophenone and benzophenone oxime. From Eq. 5, R_{a1} is the slope of the calibration plots of absorption ratio vs concentration ratio. According to the plot in Figure S7, R_{a1} for the reactant and product in oximation reaction is 1.8.
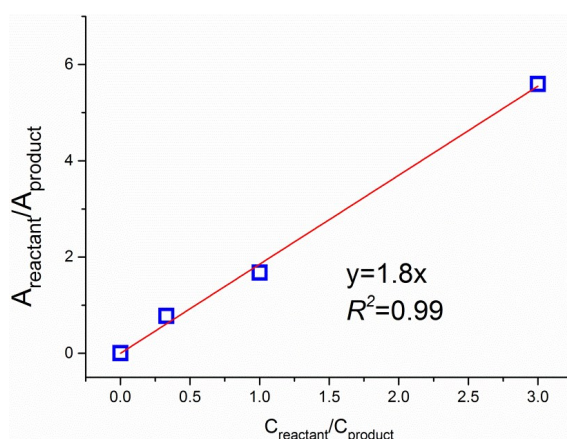

Figure S7. Standard calibration plots for absorption ratio vs. concentration ratio of reactant and product for oximation reaction obtained by HPLC-DAD.

In our experiment, the concentration of hydroxylamine was kept 20 times higher than that of benzophenone so that the oximation reaction takes place as a pseudo first-order reaction. The reaction rate constant k can be derived by plotting $\ln(C_t/C_0)$ vs time as following Eq. 6.

$$\ln\frac{C_t}{C_0} = -kt + b \qquad (6)$$

Two-phase oxidation reaction

The remaining concentration of reactant (4-methoxybenzyl alcohol) at a certain reaction t was calculated as follows. It should be noted that for this reaction in bulk phase, the following Eq. 7 can be used to calculated the remaining concentration of reactant in the "initial-rate region" because the other

side reactions have not taken place.

$$\frac{A_{alcohol}}{A_{aldehyde}} = \frac{C_t \times R_{a2}}{C_0 - C_t} \qquad (7)$$

where $A_{alcohol}$ and $A_{aldehyde}$ represent UV absorption of reactant (4-methoxybenzyl alcohol) and product (4-methoxybenzaldehyde) at the detection wavelength of 254 nm; C_0 and C_t represent the initial concentration and remaining concentration of reactant (4-methoxybenzyl alcohol); R_{a2} represents the ratio of absorption efficiency of 4-methoxybenzyl alcohol and 4-methoxybenzaldehyde.

$$\frac{A_{alcohol}}{A_{aldehyde}} = \frac{C_{alcohol}}{C_{aldehyde}} R_{a2} \qquad (8)$$

$C_{alcohol}$ and $C_{aldehyde}$ are the concentrations of 4-methoxybenzyl alcohol and 4-methoxybenzaldehyde. According to the plot in Figure S8 and Eq. 8, R_{a2} for the reactant and product in two-phase oxidation reaction is identified to be 0.07.
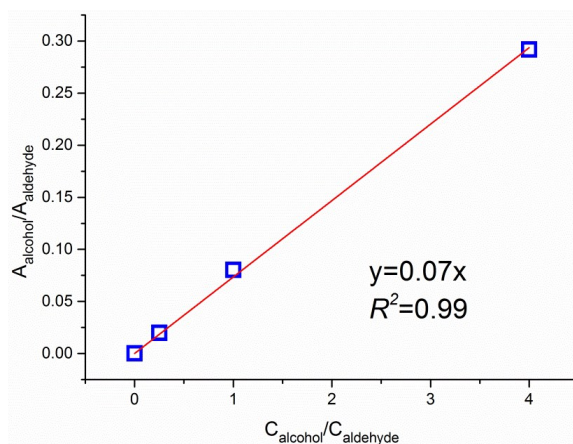

Figure S8. Standard calibration plots for absorption ratio vs. concentration ratio of reactant and product for two-phase oxidation reaction obtained by HPLC-DAD.
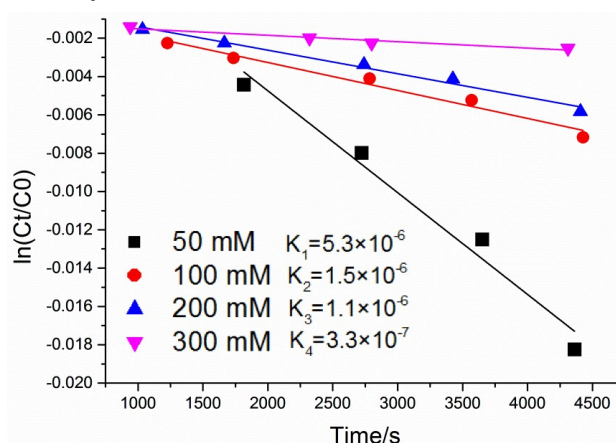

Figure S9. Plots for $\ln(C_t/C_0)$ vs time for two-phase oxidation reaction in bulk phase with 4-methoxybenzyl alcohol at different initial concentrations (50 mM, 100 mM, 200 mM, and 300 mM).

In our experiment, the concentration of sodium hypochlorite (NaClO) was much higher than that of 4-methoxybenzyl alcohol for this heterogeneous reaction. The relationships between $\ln(C_t/C_0)$ and

time with 4-methoxybenzyl alcohol at different initial concentrations in Figure S9 indicate that the reaction rate constant changed with the initial reactant concentration, and thus this heterogeneous reaction is not a zeroth-order reaction. Consequently, this two-phase reaction should take place as a pseudo first-order reaction. The reaction rate constant k can be derived by plotting $\ln(C_t/C_0)$ vs time as following Eq. 9.

$$\ln \frac{C_t}{C_0} = - kt + b \tag{9}$$

Eschenmoser coupling reaction

The concentration of enaminone product **11** (C_{11}^t) at a certain reaction t was calculated as follows.

$$\frac{A_9}{A_{11}} = \frac{C_9^t \times R_{a3}}{C_{11}^t} = \frac{(C_9^0 - C_{11}^t) \times R_{a3}}{C_{11}^t} \tag{10}$$

where A_9 and A_{11} represent UV absorption of reactant **9** (1-methylpyrrolidine-2-thione) and product **11** at the detection wavelength of 280 nm; C_9^0 and C_9^t represent the initial concentration and remaining concentration of reactant **9** (1-methylpyrrolidine-2-thione); R_{a3} represents the ratio of absorption efficiency of reactant **9** (1-methylpyrrolidine-2-thione) and product **11** (enaminone).

$$\frac{A_9}{A_{11}} = \frac{C_9}{C_{11}} R_{a3} \tag{11}$$

C_9 and C_{11} are the concentrations of reactant **9** and product **11**. From Eq. 11, R_{a3} is the slope of the calibration plots of ion intensity ratio vs concentration ratio. According to the plot in Figure S10, R_{a3} for the reactant **9** and product **11** in the Eschenmoser coupling reaction is 0.24.
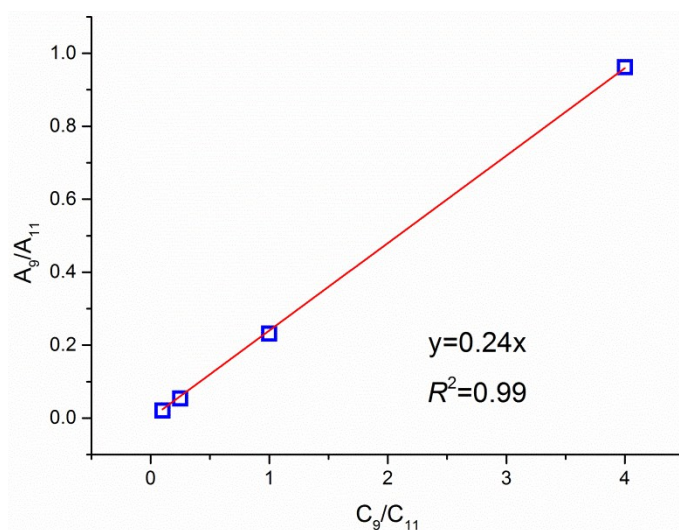

Figure S10. Standard calibration plots for ion intensity ratio vs. concentration ratio of reactant **9** and product **11** for the Eschenmoser coupling reaction obtained by by HPLC-DAD.

In our experiment, the Eschenmoser coupling reaction takes place as a second-order reaction, but the initial concentrations of 1-methylpyrrolidine-2-thione (reactant **9**) and diethyl bromomalonate (reactant **10**) were different. The initial concentrations of 1-methylpyrrolidine-2-thione (reactant **9**) and diethyl bromomalonate (reactant **10**) were represented by C_9^0 and C_{10}^0. The reaction rate constant k can

be derived by plotting $\dfrac{1}{C_9^0 - C_{10}^0} ln \dfrac{C_9^0 - C_{11}^t}{C_{10}^0 - C_{11}^t}$ vs time as following Eq. 12.

$$\frac{1}{C_9^0 - C_{10}^0} ln \frac{C_9^t}{C_{10}^t} = \frac{1}{C_9^0 - C_{10}^0} ln \frac{C_9^0 - C_{11}^t}{C_{10}^0 - C_{11}^t} = kt + b \tag{12}$$

Compared with bulk reaction, acceleration factor (AF) in the ultrasonic nebulization generated microdroplet reactions was identified as the ratio of the reaction rate constant in UN microdroplets and that in bulk phase (k_{HUN} vs k_{bulk}) (Eq. 13). The yield can be calculated based on Eq. 14.

$$AF = \frac{k_{HUN}}{k_{bulk}} \tag{13}$$

$$Y_{calculated} = \frac{C_0 - C_t}{C_0} \ or \ \frac{C_{11}^t}{C_9^0} \tag{14}$$

Section 5: The side reactions of two-phase oxidation reaction in the bulk phase

There were side reactions in the two-phase reaction between 4-methoxybenzyl alcohol in EtOAc and aqueous NaClO in bulk phase. As shown in Figure S11, after 421 min, the bulk reaction generated abundant 3-chloro-4-methoxybenzaldehyde (**C**) and 4-chloroanisole (**D**) in addition to 4-methoxybenzaldehyde (**B**), the expected oxidation product. As shown in Figure S12 and S13, the structures of byproducts **C** and **D** were identified by GC-MS and ^{1}H NMR. According to the temporal peak area profiles of the reactant (**A**) and products (**B**, **C** and **D**) obtained by HPLC for the bulk phase reaction (Figure S14), the presumed reaction pathways were shown in Scheme S1. In the initial stage, reaction of 4-methoxybenzyl alcohol with NaClO resulted in 4-chloroanisole (**D**) through ipso substitution in addition to the oxidation product, 4-methoxybenzaldehyde (**B**), which is consistent with previous report.[2] Then the chlorination reaction of the newly formed 4-methoxybenzaldehyde (**B**) with

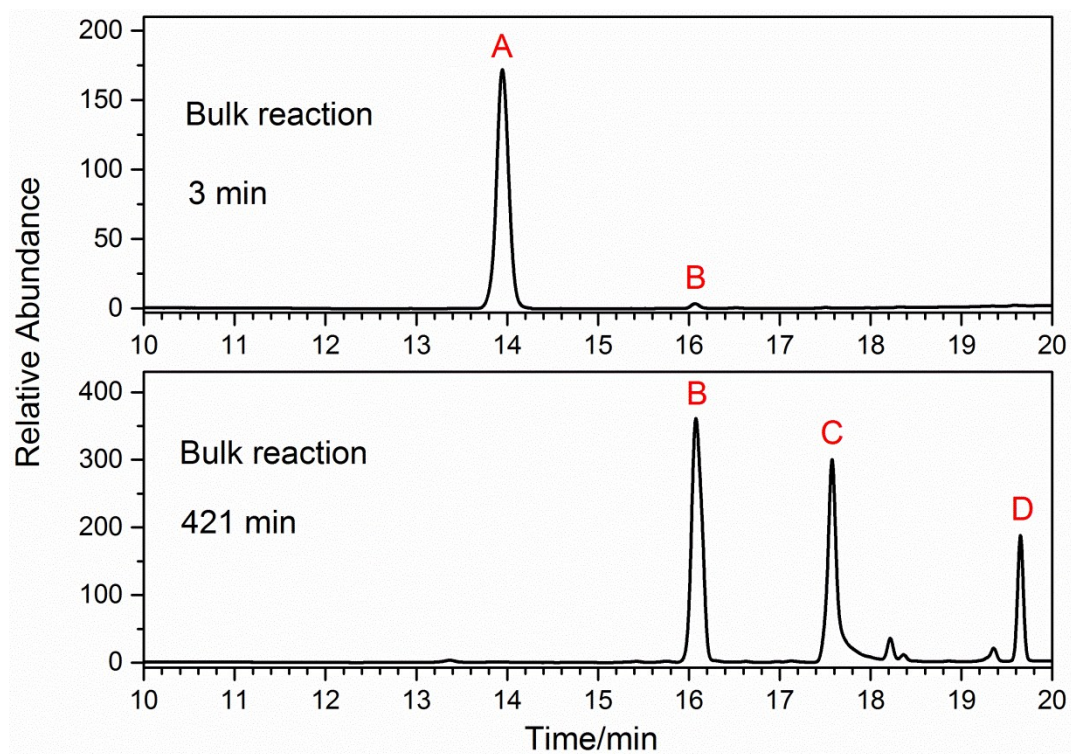NaClO generated 3-chloro-4-methoxybenzaldehyde (**C**).[3]

Figure S11. HPLC chromatograms of the reaction solution of two-phase oxidation reaction in the bulk phase at different reaction time. For HPLC analysis, 50 μL ethyl acetate fraction was diluted 20-fold with ethyl acetate. (Peak identity: **A**, 4-methoxybenzyl alcohol; **B**, 4-methoxybenzaldehyde; **C**, 3-chloro-4-methoxybenzaldehyde; **D**, 4-chloroanisole)
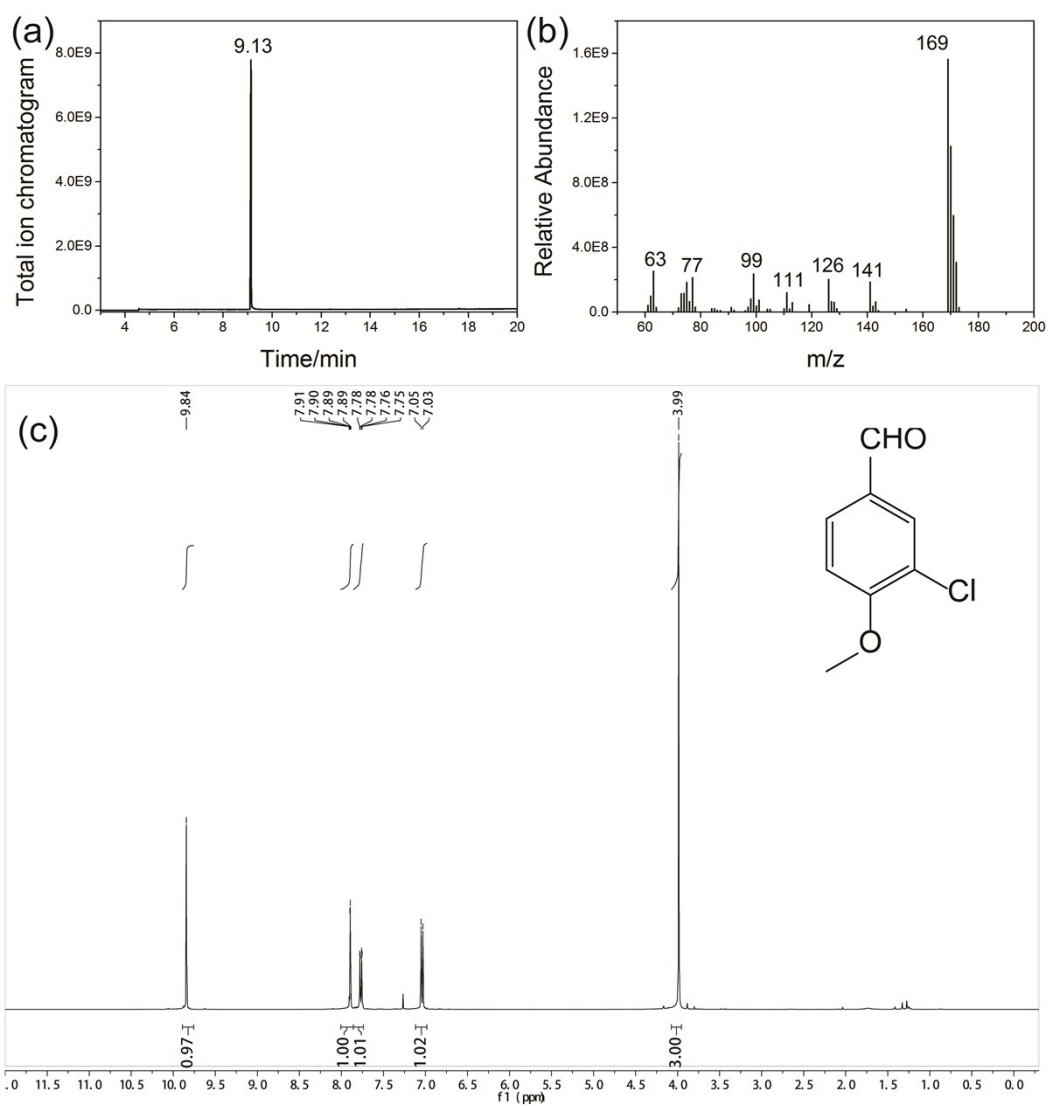
Figure S12. The total ion chromatogram of GC-MS (a), EI mass spectrum at 9.13 min (b) and ^{1}H NMR (c) of compound **C** after column chromatography separation on silica gel.
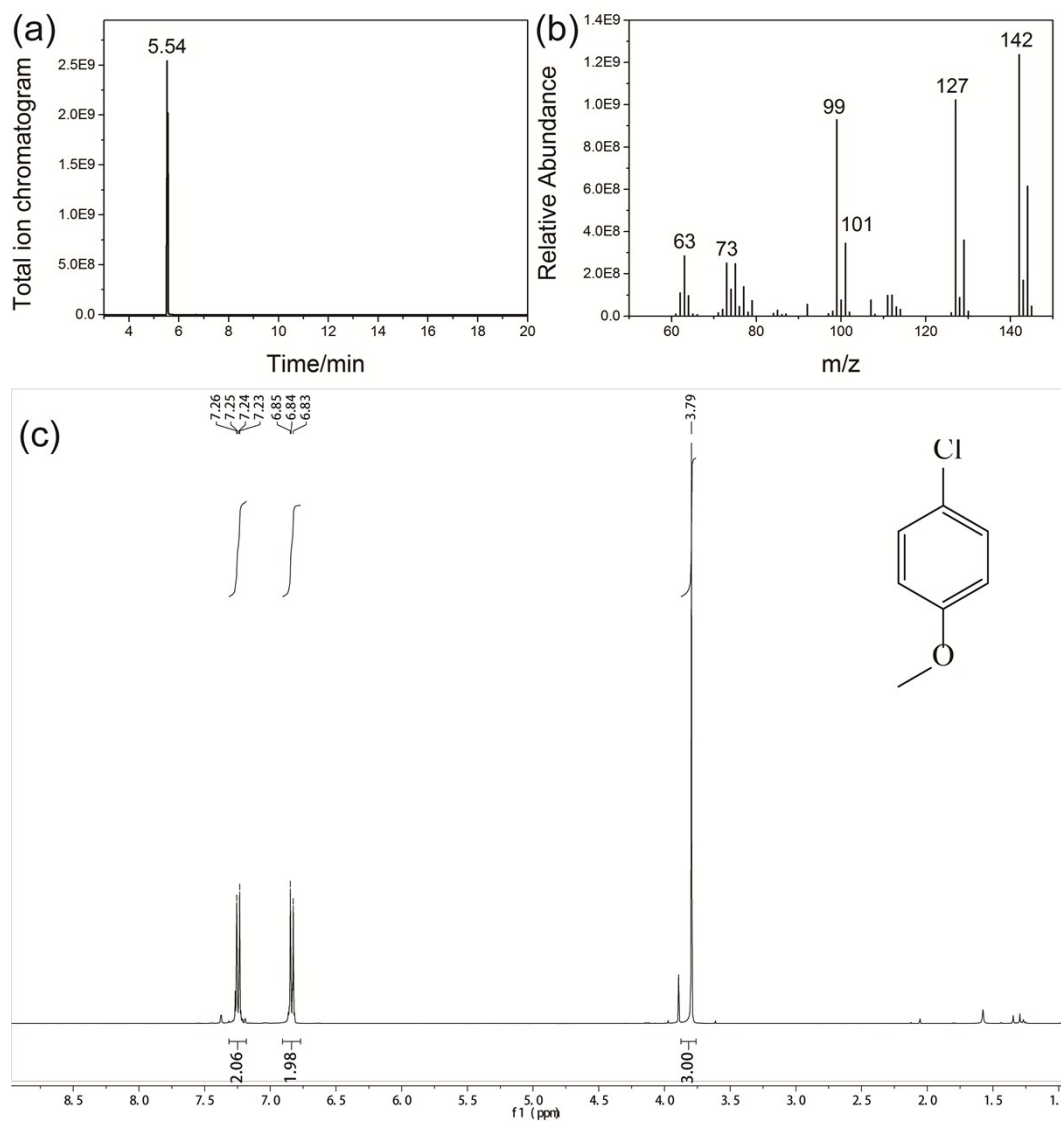
Figure S13. The total ion chromatogram of GC-MS (a), EI mass spectrum at 5.54 min (b) and ^{1}H NMR (c) of compound **D** after column chromatography separation on silica gel.
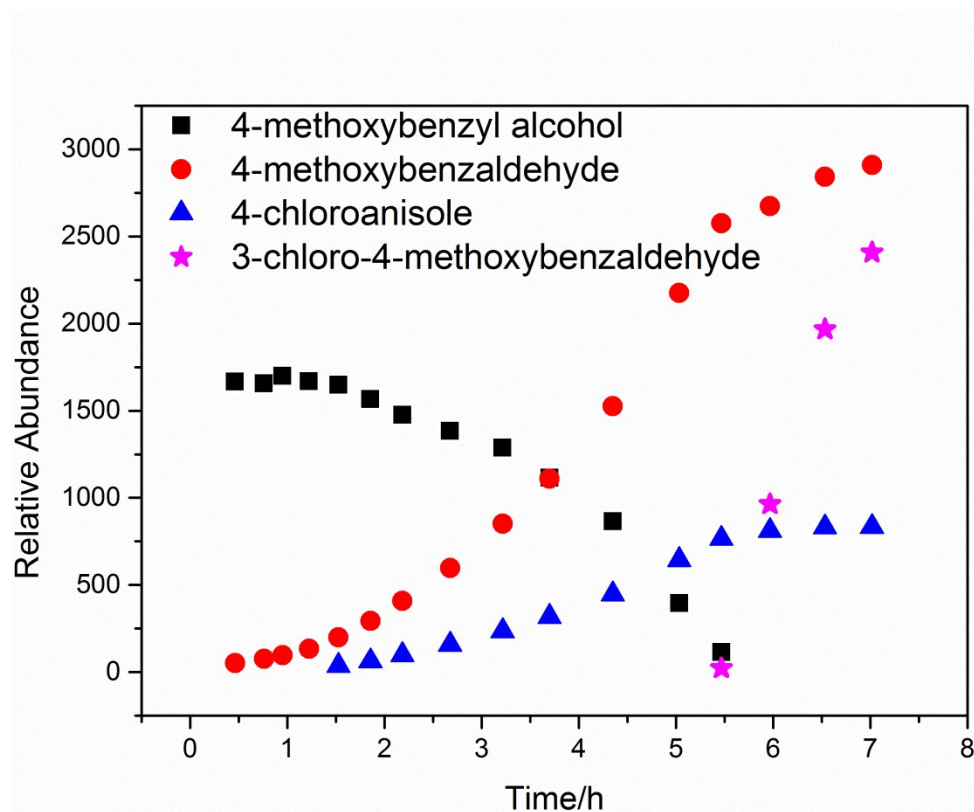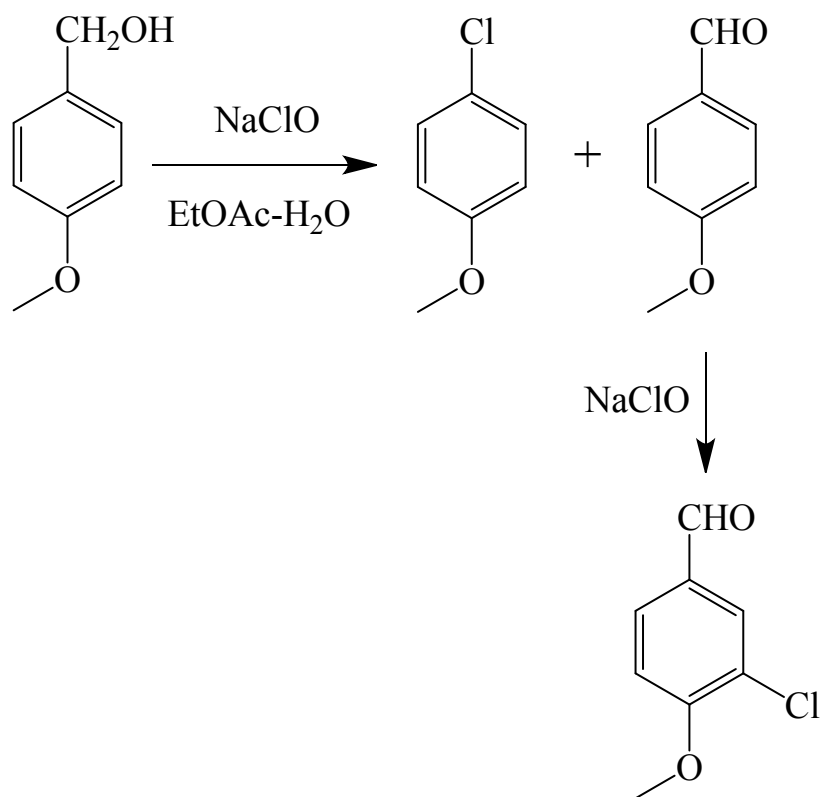
Figure S14. Plots of the peak area of reactant (4-methoxybenzyl alcohol) and products (4-methoxybenzaldehyde, 3-chloro-4-methoxybenzaldehyde and 4-chloroanisole) vs. time in the bulk two-phase oxidation reaction.

Scheme S1. Proposed reaction pathways of the two-phase reaction in bulk phase
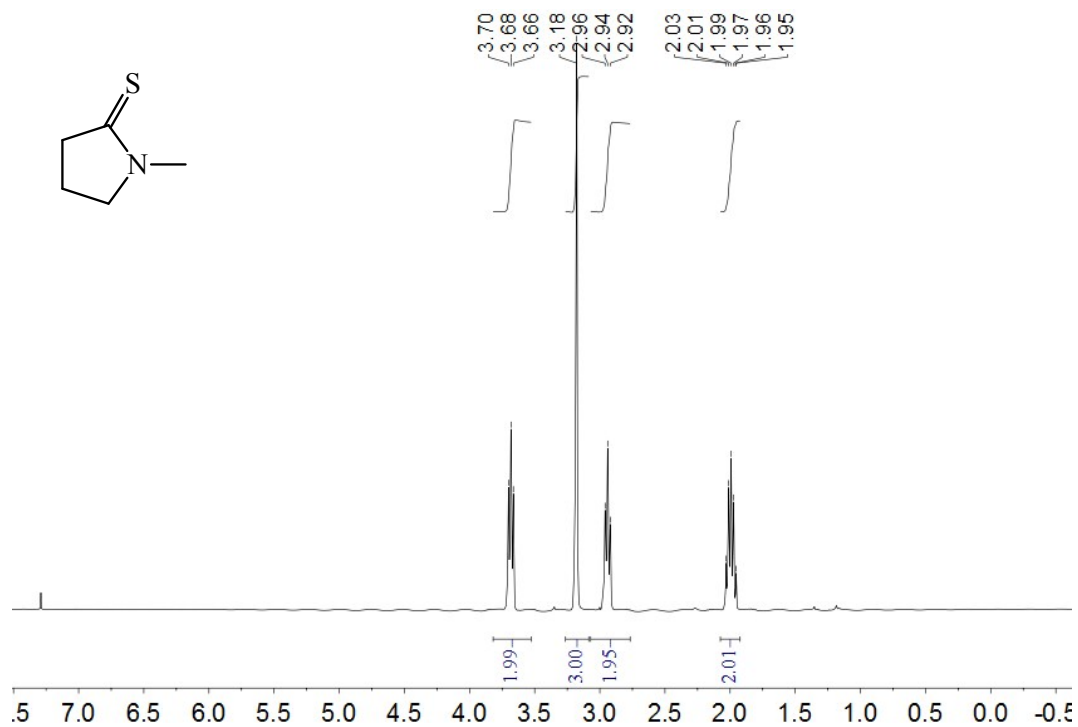
Section 6: NMR for Eschenmoser coupling reaction

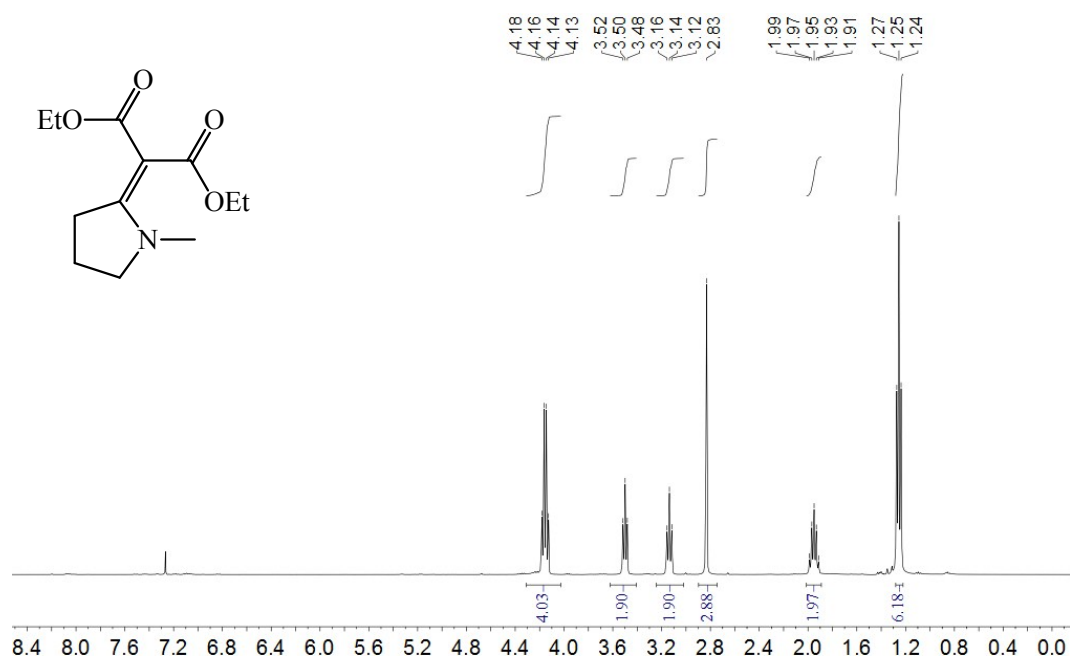**Figure S15.** The ^{1}H NMR (c) of 1-methylpyrrolidine-2-thione **9**.

Figure S16. The ^{1}H NMR (c) of product **11** after column chromatography separation on silica gel is consistent with previous report.[4]

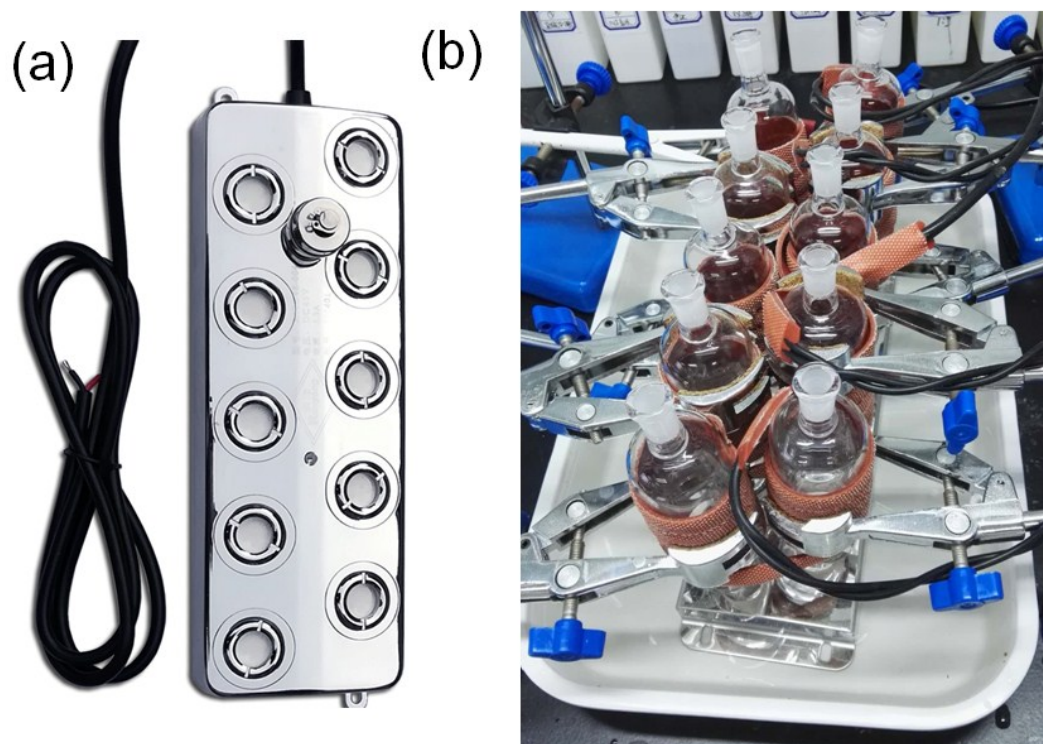# Section 7: Scale up of microdroplet reaction

Figure S17. (a) An industrial nebulization plate with 10 ultrasonic nebulizers and (b) the scale-up setup for HUN microdroplet reaction

References:

1. N. D. Koduri, H. Scott, B. Hileman, J. D. Cox, M. Coffin, L. Glicksberg and S. R. Hussaini, *Organic letters*, 2011, 14, 440-443.

2. H. V. Carrillo, A. Y. Rodriguez, R. G. Landolt and W. H. Hendrickson, *Synlett*, 2011, 22, 2069-2071.

3. A. T. Lebedev, G. M. Shaydullina, N. A. Sinikova and N. V. Harchevnikova, *Water Res.*, 2004, 38, 3713-3718.

4. N. D. Koduri, B. Hileman, J. D. Cox, H. Scott, P. Hoang, A. Robbins, K. Bowers, L. Tsebaot, K. Miao and M. Castaneda, *RSC Adv.*, 2013, 3, 181-188.